

The anatomy of the simplest Duflo-Zuker mass formula

Joel Mendoza-Temis,¹ Jorge G. Hirsch,¹ and Andrés P. Zuker²

¹ *Instituto de Ciencias Nucleares, Universidad Nacional
Autónoma de México, 04510 México, D.F., Mexico*

² *IPHC, IN2P3-CNRS, Université Louis Pasteur, F-67037 Strasbourg, France*

Abstract

The simplest version of the Duflo-Zuker mass model (due entirely to the late Jean Duflo) is described by following step by step the published computer code. The model contains six macroscopic monopole terms leading asymptotically to a Liquid Drop form, three microscopic terms supposed to mock configuration mixing (multipole) corrections to the monopole shell effects, and one term in charge of detecting deformed nuclei and calculating their masses. A careful analysis of the model suggests a program of future developments that includes a complementary approach to masses based on an independently determined monopole Hamiltonian, a better description of deformations and specific suggestions for the treatment of three body forces.

PACS numbers: 21.10.Dr

Keywords: Nuclear masses, binding energies, mass models, Duflo-Zuker, three body forces.

I. INTRODUCTION

Masses are a fundamental property of nuclei, whose accurate knowledge is important for a large number of processes in nuclear physics, in particular in astrophysical phenomena [1], and for a variety of applications in other areas, from elementary particle physics to a precise determination of the kilogram. Though much progress has been made in measuring the masses of exotic nuclei (see for example Ref.[2] and references therein), theoretical models are still necessary to *predict* them in regions far from stability [3]. Advances in the calculation of atomic masses have been hampered by the absence of a full theory of the nuclear interaction and by the difficulties inherent to quantum many-body calculations. There has been much work in developing mass formulas with either microscopic and macroscopic input or within a fully microscopic framework.

Soon after the latest compilation of nuclear masses AME03 [4] was published, a comparison between the predictions of a large set of mass models, which were fitted to describe the nuclear masses included in AME95 [5], for the more than 300 new masses included in AME03 was presented [3]. It became evident that the predictions of the Duflo-Zuker (DZ) model [6] were outstanding. Recent tests of the predictive power of nuclear models [7] confirm the ability of DZ to make stable predictions which are more accurate than those offered by other models.

The model has many parameters: 28 in the original version, tabulated by Audi [8] and used in the comparisons [3]. The code is unpublished but a version with up to 33 parameters circulates and it is now available in [8]. Another code, with only 10 parameters (DZ10) [8] leads to good though less spectacular results but embodies the essence of the model.

Our task is to examine in full detail what DZ10 does and as we go point to possible ways to improve on it, based on what has been learned in recent years. To anticipate on what follows: Of the ten terms enumerated in the abstract the three—crucial ones—supposed to represent configuration mixing are anomalous in the sense that they contain three body effects of unknown origin and they scale with the total number of particles A instead of $A^{1/3}$ as shell effects should. They will be examined in special detail.

In Section II the basic elements of the DZ10 model are described. Section III deals with the evolution of the results as the ten parameters of the fits are switched on; the origin of the anomalous scaling becomes apparent. Predictive power and stability of the model

are examined in Section IV. An analysis of the action of the anomalous terms follows in Section V. A full explanation of their nature is given in Section VI by comparing the macroscopic terms with an independently determined monopole Hamiltonian. Section VII is devoted to the need to introduce three body forces. Section VIII is the conclusion and an homage to Jean Duflo.

II. BASIC ELEMENTS

To illustrate what a model of nuclear masses is supposed to do consider Fig.1 where experimental binding energies of even-even nuclei are subtracted from an improved version of the Bethe-Weizsäcker liquid drop (LD) form, given in Eq.(1) for Z protons, and N neutrons, with mass number $A = N + Z$ and isospin $T = |N - Z|/2$. The asymmetry term is generalized to include Wigner and surface contributions. Only even-even nuclei are shown as they contain all the basic information. The pairing term is omitted leading to (mostly) positive definite shell effects.

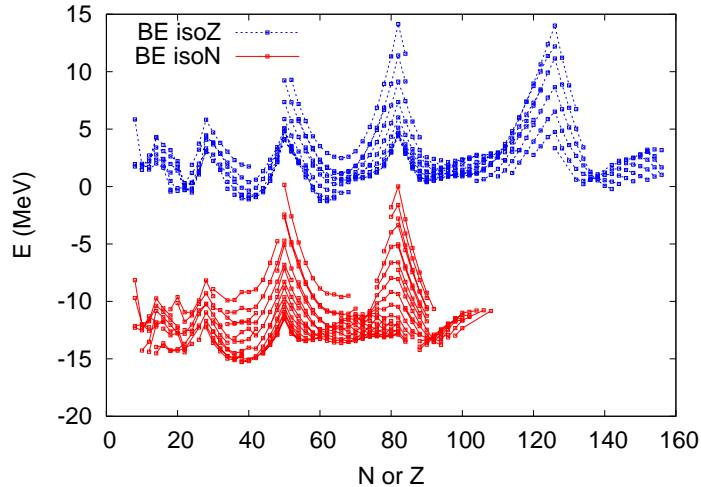


FIG. 1: Shell effects ($BE(\text{exp})-E(\text{LD})$) along isotope and isotone lines (latter displaced by -14 MeV). Only even-even nuclei are shown.

$$E(\text{LD}) = 15.5A - 17.8A^{2/3} - 28.6\frac{4T(T+1)}{A} + 40.2\frac{4T(T+1)}{A^{4/3}} - \frac{.7Z(Z-1)}{A^{1/3}}. \quad (1)$$

Both graphs contain exactly the same information. Four remarks (injunctions):

- **LD** Any model must contain the LD either explicitly or asymptotically.

- **EI** The only observed closures worth considering are the “extruder-intruder” (EI) ones at $N, Z = (14), 28, 50, 82$ and 126 , in which the subshell of largest angular momentum is “extruded” from harmonic oscillator (HO) shell of principal quantum number p and becomes the intruder in the $p - 1$ HO shell.
- **SPH-DEF** Flat patterns at the bottom of Fig.1, as in the regions $90 < N < 110$ and $60 < Z < 75$, correspond to well deformed nuclei. Any model must treat them specifically.
- **$A^{1/3}$** . Shell effects—defined by subtracting any contribution to the total binding energy from its asymptotic form—should scale as $A^{1/3}$.

These injunctions were incorporated in steps. First came the purely phenomenological work of Duflo [9]. It was based on simple algebraic forms that fitted masses with RMSD of some 350 keV. However, it extrapolated poorly. In a companion paper [10] it was shown that the algebraic simplicity could be reconciled with a microscopic derivation provided the microscopic shell effects be separated from the macroscopic (LD) form. Then the observed closures were taken to define conventional shell model spaces and it was shown that configuration mixing would lead to simple quadratic and quartic forms in the number of valence particles [10]. The trouble was that the observed closures had to be put by hand. The breakthrough came by incorporating hints from [11] showing that from realistic interactions one could extract a “master term” containing both the leading LD bulk energy and strong harmonic oscillator (HO) shell effects. It was left to shift the HO closures to the observed ones and then use the shell model forms derived in [10] to mock configuration mixing. In a recent paper [12] the DZ strategy is presented in some detail, stressing in particular that it is not a “mass formula” but a functional of the orbital occupancies and explaining its success in dealing with well deformed nuclei. Our aim here is to show how to incorporate the last injunction above, by unearthing the reasons why DZ fails to respect it, which we (cryptically) anticipate with the benefit of hindsight: DZ assumed that asymptotic behaviour involves an LD form which ignores $A^{1/3}$ terms that turned out to be present and treated as genuine shell effects. Next section starts dealing with the problem.

A. The Master term

In DZ [6] it was assumed (guessed) that realistic two body interactions generate two collective terms solely responsible for the leading LD contributions, of the form

$$M_A = \frac{\hbar\omega}{\hbar\omega_0} \left(\sum_p \frac{m_p}{\sqrt{D_p}} \right)^2, \quad M_T = \frac{\hbar\omega}{\hbar\omega_0} \left(\sum_p \frac{t_p}{\sqrt{D_p}} \right)^2 \quad (2)$$

where $\hbar\omega$ is the HO frequency, $\hbar\omega_0$ is left as a free parameter, $D_p = (p+1)(p+2)$ is the degeneracy of the major HO shell of principal quantum number p , $m_p = n_p + z_p$, $t_p = n_p - z_p$, where n_p, z_p are number operators for neutrons and protons, respectively.

To obtain asymptotic estimates for M_A we assume at first $N = Z$ and, following Ref. [13], sum up to the closed Fermi shell p_f , which we associate to the total number of particles A through (use $p^{(3)} = p(p-1)(p-2)$; \implies leads to, implies; \approx approximately; \therefore therefore)

$$A = \sum_p m_p = \sum_{p=0}^{p_f} 2D_p = \frac{2(p_f+3)^{(3)}}{3} \approx \frac{2(p_f+2)^3}{3} \implies (p_f+2) \approx \left(\frac{3}{2}A\right)^{1/3} \quad (3)$$

Next we estimate $\hbar\omega$ by relating it to the observed square radius [13],

$$\langle r^2 \rangle = \frac{\hbar}{AM_{nucl}\omega} \sum_p m_p(p+3/2) \approx \frac{3\hbar}{4M_{nucl}\omega} (p_f+2) \therefore \hbar\omega = 35.59 \frac{A^{1/3}}{\langle r^2 \rangle} \text{MeV}. \quad (4)$$

where M_{nucl} is the nucleon mass. The 35.59 coefficient follows from an accurate estimate of the nuclear radii of magic and semimagic nuclei [14], which may serve as a reminder of the need to incorporate an isospin dependence,

$$\sqrt{\langle r_{\nu\pi}^2 \rangle} \approx A^{1/3} \left(.943 - 0.4 \frac{t}{A^{4/3}} - 0.34 \left(\frac{t}{A} \right)^2 \right) e^{(1.04/A)}; \quad t = N - Z. \quad (5)$$

In what follows, whenever convenient, we shall replace $\hbar\omega/\hbar\omega_0$ or $\hbar\omega$ by the scaling factor $1/\rho$ suggested by Eq (4), where

$$\rho = \langle r^2 \rangle / A^{1/3} = A^{1/3} \left[1 - 0.5 \left(\frac{t}{A} \right)^2 \right]^2. \quad (6)$$

retaining the DZ10 choice for $\langle r^2 \rangle$ rather than the more sophisticated Eq. (5).

Approximating $\sqrt{D_p} \approx p + 3/2$, leads to

$$\sum_p \frac{m_p}{\sqrt{D_p}} = \sum_p 2\sqrt{D_p} \approx p_f(p_f+4) \approx (p_f+2)^2 \quad (7)$$

$$M_A = \frac{1}{\rho} \left(\sum_p \frac{m_p}{\sqrt{D_p}} \right)^2 \approx \frac{1}{\rho} (p_f+2)^4 \quad (8)$$

Similarly, for N and Z separately (\equiv equivalent)

$$N \approx \frac{(p_{f\nu} + 2)^3}{3}, \quad Z \approx \frac{(p_{f\pi} + 2)^3}{3}, \quad (9)$$

$$M_N \equiv \frac{1}{\rho} \left(\sum_p^{p_{f\nu}} \frac{n_p}{\sqrt{D_p}} \right)^2 \approx \frac{(p_{f\nu} + 2)^4}{4\rho} \approx \frac{(3N)^{4/3}}{4A^{1/3}}, \quad (10)$$

$$M_Z \equiv \frac{1}{\rho} \left(\sum_p^{p_{f\pi}} \frac{z_p}{\sqrt{D_p}} \right)^2 \approx \frac{(p_{f\pi} + 2)^4}{4\rho} \approx \frac{(3Z)^{4/3}}{4A^{1/3}}, \quad (11)$$

where $p_{f\nu}$, $p_{f\pi}$ are the neutron and proton Fermi levels. As

$$M_A = M_Z + M_P + 2\sqrt{M_Z}\sqrt{M_P}, \quad M_T = M_Z + M_P - 2\sqrt{M_Z}\sqrt{M_P}, \quad (12)$$

the leading asymptotic (\asymp) estimates in t/A become

$$M_A \asymp \left(\frac{3}{2}\right)^{4/3} A \left(1 - \frac{2}{9} \left(\frac{t}{A}\right)^2\right); \quad M_T \asymp \left(\frac{3}{2}\right)^{4/3} A \left(\frac{2t}{3A}\right)^2 \quad (13)$$

To go beyond leading order is delicate, but combining Eqs. (3) and (7) we find that $A^{4/3}$ goes as $p_f^4 + 8p_f^3 + 23p_f^2 + \dots$ against $p_f^4 + 8p_f^3 + 16p_f^2$ for $(\sum_p m_p D_p^{-1/2})^2$, which points to a substantial $A^{1/3}$ ($\approx p_f + 2$) contribution to M_A but a vanishing one in $A^{2/3}$. In other words—as it stands—the master term has no contribution to the LD surface energy. To look for its possible origin we examine the microscopic derivation of M_A .

B. Origin of the master terms. Scaling

Let us rely on the general factorization property for arbitrary quadratic forms [11]

$$\sum_{x,\alpha} V_{x\alpha} \Omega_x \cdot \Omega_\alpha = \sum_\mu E_\mu \left(\sum_k \Omega_k U_{k\mu} \sum_\beta \Omega_\beta U_{\beta\mu} \right), \quad (14)$$

which we specialize to the monopole part of the Hamiltonian (detailed discussion in [15]), in which case V are symmetric matrices, diagonalized by unitary transformations U and Ω stand for isoscalar (number m), or isovector (isospin T) operators. To fix ideas consider the result of diagonalizing the isoscalar monopole interaction for the first 8 major oscillator shells for the chiral N3LO interaction [16] smoothed by the $V_{\text{low } k}$ procedure [17]. There are 36 subshells and as many eigenvalues. One of them turns out to be strongly dominant.

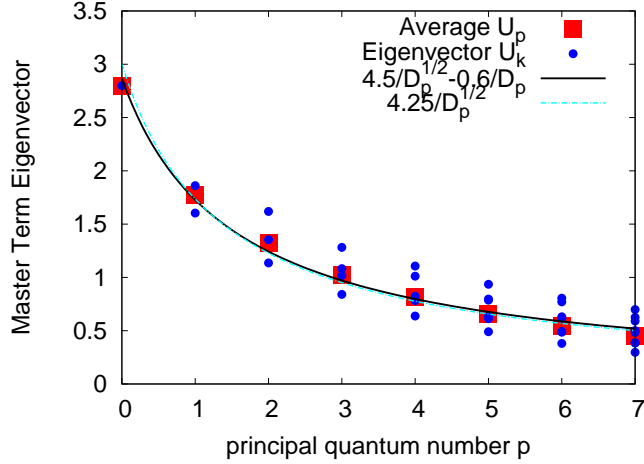


FIG. 2: The isoscalar master eigenvector (boosted by an arbitrary factor) for the N3LO interaction. According to Eq. (15) only the average term in U_p contributes to the closed major shells.

Within a very good approximation its value is proportional to $\hbar\omega \equiv 1/\rho$ and its eigenvector is independent of it. The corresponding factor in Eq. (14) can be split as

$$\sum_k m_k U_k = m_p U_p + \sum_k m_k (U_k - U_p), \quad U_p = \frac{\sum_k D_k U_k}{D_p}, \quad \sum_k D_k = \sum_k (2j_k + 1) = D_p, \quad (15)$$

where j_k is the angular momentum of subshell k . Only the term in U_p survives when the major shell is full. It defines the collective monopole operator in full analogy with its multipole counterparts such as pairing and quadrupole and, again, in analogy with them [11, 15] we expect $U_p \propto D_p^{-1/2}$ (\propto proportional to). The calculated U_p are rescaled by a factor six so as to make them of order unity and two fits are made to the $t = 0$ patterns, yielding $U_p = 4.25D_p^{-1/2}$, and a variant $U_p^v = 4.47D_p^{-1/2} - 0.6D_p^{-1}$, which are seen to be almost undistinguishable in Figure 2. However, the asymptotic contributions to the master term are quite different $M_A \simeq 17.06A - 20.97A^{1/3}$ and $M_A^v \simeq 17.27A - 10.51A^{2/3} - 5.64A^{1/3}$. They will be referred to as “asymptotics” for short, to distinguish them from “shell effects”. In the first panel of Fig. 3 it is seen that both approximations produce nearly the same shell effects that show as parabolic segments bounded by HO closures at $N = 8, 20, 40, 70, 112$ and 168 . A remarkable result, in view of the very different asymptotics. Each segment can be represented by the form $m_p(m_p - D_p)(D_p\rho)^{-1}$, where the denominator ensures at midshell ($m_p = D_p/2$) an amplitude $D_p/4\rho \propto A^{1/3}$. To check that this is the correct scaling, in the second panel of Fig. 3 the master shell effects of the first panel are subject to an

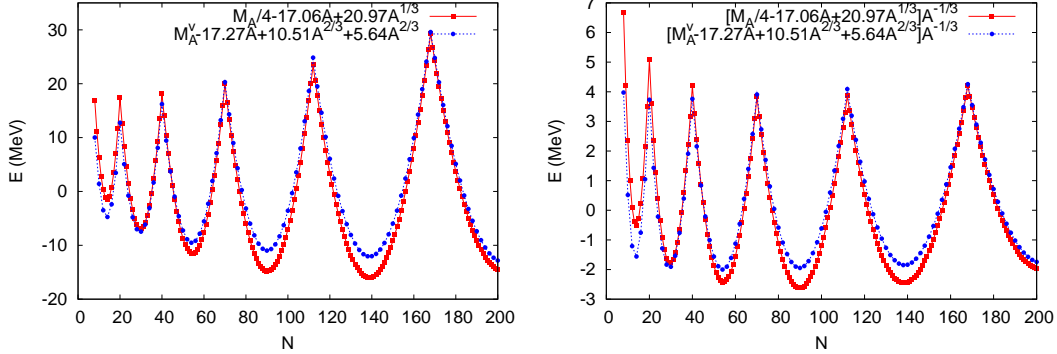


FIG. 3: Master shell effects produced by M_A and M_A^v for $t = N - Z = 0$. See text.

$A^{-1/3}$ compression. It is seen that the amplitudes become constant beyond $N, Z \approx 70$. The deviations from perfect (uniform) scaling may have consequences that deserve a comment.

Scaling is an asymptotic notion: $p + 2$ and, say, $p - 3$ both scale as $A^{1/3}$ but are quite different for small p . They differ in a “unit scaling”, *i. e.*, a factor that goes asymptotically as unity, in our example $(p - 3)/(p + 2)$. The difference between the two approximations to U_p in Figure 2 are of the same type. Fig. 3 provides another instance of the possible origin of unit scalings, which in DZ work are often represented by surface terms: typically an operator Γ affected by some unit scaling is replaced by $\Gamma(1 + \alpha/\rho)$. More generally one may consider rational functions *i. e.*, quotients of polynomials of the same rank in p (avoiding vanishing denominators, as in Eqs.(18) in next section).

C. The HO-EI transition

In the DZ implementations the combination $M \rightarrow M_A + M_T$ is employed, explicitly

$$M = \frac{1}{2\rho} \left[\left(\sum_p \frac{m_p}{\sqrt{D_p}} \right)^2 + \left(\sum_p \frac{t_p}{\sqrt{D_p}} \right)^2 \right], \quad (16)$$

while the asymmetry terms are represented by $4T(T + 1)/A$, ($T = |t|/2$) with the shell effects in M_T simply ignored. This neglect deserves reexamination and here we only note the asymptotically correct form in $T(T + 1)$ rather than T^2 is both theoretically sound and empirically significant.

The M term raises one of the outstanding problems in nuclear physics: realistic interactions fail to produce the observed closures [18], which contradicts the basic tenet of the

discipline that they are due to the spin-orbit force: what the famous $l \cdot s$ term does is to make the orbit with largest angular momentum ($j(p)$) the lowest in shell p . This term is indeed present in the realistic potentials and it suggests the correct magic numbers but it does not produce them [18]. The necessary mechanism has to be invented. Figure 4 indicates

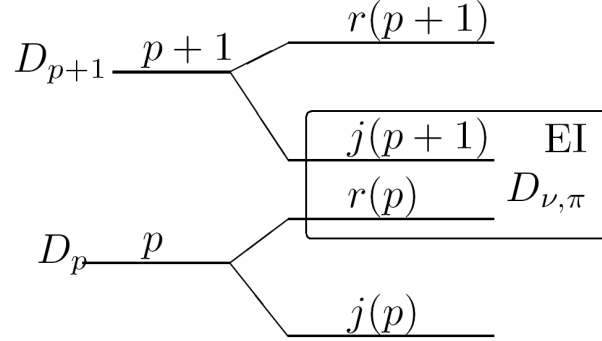


FIG. 4: Harmonic oscillator and extruder-intruder (EI) shells.

what has to be done: To change the HO closures (at $N, Z=8, 20, 70 \dots$), into the observed extruder-intruder (EI) ones at $N, Z=28, 50, 82$ and 126 . As made clear by Fig. 1 these are the only obvious ones. Therefore, the only relevant operators must separate orbit $j(p)$ of degeneracy $D_{j(p)} = 2(p+1)$ from its partners $r(p)$ of degeneracy $D_{r(p)} = p(p+1)$. The only one body operators that do it properly are

$$s_{\nu p} = \left[\frac{pn_{j_p} - 2n_{r_p}}{2(p+1)} \right], \quad s_{\pi p} = \left[\frac{pz_{j_p} - 2z_{r_p}}{2(p+1)} \right], \quad (17)$$

because they vanish at HO closures and therefore give no asymptotic LD contribution. The $2(p+1)$ denominator is arbitrary, ν and π stand for neutron and proton orbits, n and z for neutron and proton numbers. Duflo invented the following operator

$$\begin{aligned} S_{\nu} &= \sum_p^{p_{\nu}} s_{\nu p} \frac{p^2 + 4p - 5}{\sqrt{D_p}(p+2)} + \sum_p^{p_{\nu}} n_p s_{\nu p} \frac{p^2 - 4p + 5}{D_p(p+2)}, \\ S_{\pi} &= \sum_p^{p_{\pi}} s_{\pi p} \frac{p^2 + 4p - 5}{\sqrt{D_p}(p+2)} + \sum_p^{p_{\pi}} z_p s_{\pi p} \frac{p^2 - 4p + 5}{D_p(p+2)}, \\ S &= \frac{S_{\nu} + S_{\pi}}{\rho}. \end{aligned} \quad (18)$$

which represents a sophisticated example of unit scaling discussed at the end of the previous section. It leads to the remarkable result in Fig.5, where the HO peaks are practically erased to give way to EI ones, which, from left to right, correspond to $N = 74$ ($Z = 50$), $N = 82$,

$N = 106$ ($Z = 82$), $N = 126$, $N = 150$ ($Z = 126$) and $N = 184$. The choice of the $N - Z = 24$ is arbitrary.

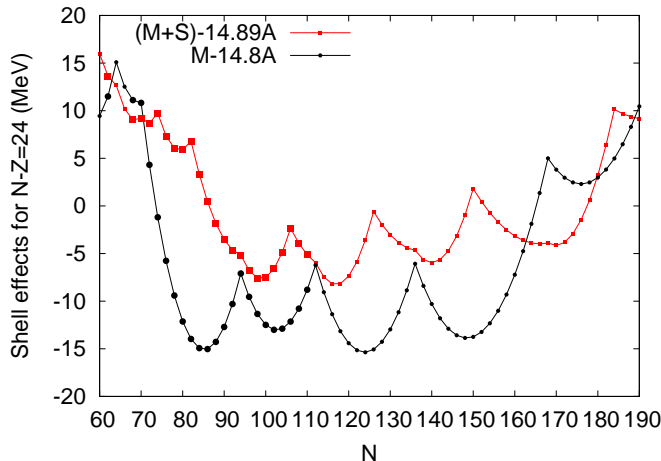


FIG. 5: The evolution from HO (dots) to EI (squares) shell effects for $N - Z = 24$ even-even nuclei. The asymptotics are roughly represented by a simple A term. Heavier marks refer to species whose masses have been measured.

D. The DZ10 equations. Macroscopic terms

The discussion in Section IIB suggests that *volume* and *surface* effects be treated in a single term but in DZ they are kept separate (which turns out to be a problem, as will be explained in the comments to Fig. 6). The terms are:

$$M + S \quad \text{and} \quad \frac{M}{\rho} \quad \text{respectively.} \quad (19)$$

The *Coulomb* term includes the charge radius r_c and a surface correction (See Ref. [14] for more sophisticated treatments)

$$V_C = \frac{Z(Z-1) + 0.76[Z(Z-1)^{2/3}]}{r_c}; \quad r_c = A^{1/3} \left[1 - \left(\frac{T}{A} \right)^2 \right] \quad (20)$$

The *asymmetry* term uses the $T(T+1)$ form, sounder than the usual $(N-Z)^2$

$$V_T = \frac{4T(T+1)}{A^{2/3}\rho}, \quad (21)$$

The *surface asymmetry* has a small unconventional part that can be viewed as the only—purely phenomenological—representative of isovector shell effects,

$$V_{TS} \equiv \frac{4T(T+1)}{A^{2/3}\rho^2} - \frac{4T(T-\frac{1}{2})}{A\rho^4}, \quad (22)$$

The *Pairing* term includes corrections of order $2T/A$:

N	Z		V_P
even	even		$(2 - 2T/A)/\rho$
even	odd	$N > Z$	$(1 - 2T/A)/\rho$
odd	even	$N > Z$	$1/\rho$
even	odd	$N < Z$	$1/\rho$
odd	even	$N < Z$	$(1 - 2T/A)/\rho$
odd	odd		$2T/(A\rho)$

Though purely phenomenological, these corrections reflect pairing effects of Coulomb and nuclear isospin breaking origin [19]. They ensure that the four mass sheets are described with equal accuracy. The $1/\rho$ scaling in $A^{-1/3}$ replaces the now deprecated $A^{-1/2}$.

The contribution to the binding energy is thus defined by six terms, of which the last four are very close to the usual LD form:

$$\langle H_m \rangle = a_1 (M + S) - a_2 \frac{M}{\rho} - a_3 V_C - a_4 V_T + a_5 V_{TS} + a_6 V_P. \quad (23)$$

E. Microscopic sector. Anomalous spherical terms

The EI spaces defined by the macroscopic (macro) sector are treated as model spaces in which to perform Shell Model calculations. The issue is discussed in Ref. [10]. Here we offer a compact summary.

To estimate the energies of an exact wavefunction $|\bar{0}\rangle$ we write it as an unperturbed part $|0\rangle$ acted upon by k -body scalar correlation operators \hat{A}_k (the evolution operator $\exp(iHt)$ is a scalar). The resulting energy has the form given in Eq.(24), where we separate a diagonal part given by the monopole Hamiltonian H_m and a correlation one involving the multipole Hamiltonian H_M [11, 15]. Both H_m and H_M are effective operators adapted for work in the valence spaces. Note that \hat{A}_1 cannot contribute since the space does not allow scalar

particle-hole excitations (no two orbits have the same j and parity).

$$|\bar{0}\rangle = (1 + \sum_k \hat{A}_k)|0\rangle \implies E = \langle 0|H_m|0\rangle + \langle 0|H_M \hat{A}_2|0\rangle \implies \quad (24)$$

$$\text{terms of type : macro; } \frac{m_v \bar{m}_v}{D_v \rho}; \quad \frac{m_v \bar{m}_v (m_v - \bar{m}_v)}{D_v^2 \rho}; \quad \frac{m_v^{(2)} \bar{m}_v^{(2)}}{D_v^3 \rho} \quad (25)$$

In Eq.(25) we use the notations $m_v^{(2)} = m_v(m_v - 1)$ and $\bar{m}_v = D_v - m_v$ to write the form of the possible contributions in a valence space v of degeneracy D_v . The macro term is solely responsible for the closed shells at $m_v = \bar{m}_v = 0$. The origin of the quadratic term can be both monopole (as in Fig. 3) and multipole (e. g. the pairing interaction in its simplest form). We have no argument to ascribe the cubic terms to configuration mixing. At the time the DZ model(s) were formulated the possibility that it could be due to a genuine monopole three body force was thought to be unlikely; nowadays it has become a certainty that such forces are essential. In section VI we shall find clues indicating that the quadratic term owes much to configuration mixing and that the cubic one must be due to a genuine three body force whose determinant role in the HO-EI transition will be established in Section VII. We are left with the quartic correlation term whose form is dictated by the remark that $H_M \hat{A}_2$ is a four body operator that must vanish at $m_v = \bar{m}_v = 0$ or 1 because only H_m acts at these points.

In Eq. (25) the denominators are chosen so as to ensure correct $A^{1/3}$ scalings. Unfortunately, an original error (explained in the discussion of Fig. 6) leads to the need of anomalous scalings for the ‘‘spherical’’ terms that operate in the EI valence spaces. Using ν and π indices for neutron and proton quantities, they take the form

$$s_3 = \frac{1}{\rho} \left[\frac{n_\nu \bar{n}_\nu (n_\nu - \bar{n}_\nu)}{D_\nu} + \frac{n_\pi \bar{n}_\pi (n_\pi - \bar{n}_\pi)}{D_\pi} \right], \quad (26)$$

$$s_4 = \frac{1}{\rho} \left[2^{(\sqrt{p_\pi} + \sqrt{p_\nu})} \cdot \left(\frac{n_\nu \bar{n}_\nu}{D_\nu} \right) \cdot \left(\frac{n_\pi \bar{n}_\pi}{D_\pi} \right) \right]. \quad (27)$$

leading to contributions to the binding energy

$$\langle H_s \rangle = a_7 s_3 - a_8 \frac{s_3}{\rho} + a_9 s_4. \quad (28)$$

F. Deformation term

That the onset of deformation is due to the promotion of four neutrons and four protons from an r shell to the next major HO shell is something that can be read from Nilsson

diagrams as pointed out in [10]. The loss of macroscopic (monopole) energy is upset by the gain due to the quadrupole force, simulated by a specific quartic operator (which scales correctly). Calling generically $n' = n - 4$, $\bar{n}' = \bar{n} + 4$, its form and contribution to the energy are

$$d_4 = \frac{1}{\rho} \left[\left(\frac{n'_\nu \bar{n}'_\nu}{D_\nu^{3/2}} \right) \cdot \left(\frac{n'_\pi \bar{n}'_\pi}{D_\pi^{3/2}} \right) \right], \quad \langle H_d \rangle = a_{10} d_4. \quad (29)$$

The idea was very successfully incorporated in the original DZ fits, and is at the origin of the spherical description of rotational nuclei [12, 15, 20], by now firmly established, which goes well beyond Eq. (29) and points to its limitations. The valence space involves two contiguous major HO shells in which good approximations close to Elliott's SU3 symmetry operate. Eq. (29) simulates well the mechanism at the beginning of the deformed regions by staying in the EI space where the r particles represent the lower shell and the j orbit the upper one. It fails as soon as the r orbits are full. Fig. 12 in Section V will provide an example of the problem.

III. THE FITS

Two calculations are made for each nucleus. Both include the macroscopic contribution plus either the anomalous spherical terms or the deformed one.

The a_i coefficients are varied to minimize the root mean square deviation (RMSD) between the predicted binding energies $BE_{th}(N, Z)$ and the experimental ones $BE_{exp}(N, Z)$, reported in [4], modified so as to include more realistically the electron binding energies as explained in Appendix A of Lunney, Pearson and Thibault [3]. For each nucleus a spherical and a deformed calculation are made, and the one with largest binding is selected:

$$\begin{aligned} BE_{th} &= \langle H_m \rangle + \langle H_s \rangle & \text{if } Z < 50 \\ BE_{th} &= \langle H_m \rangle + \max(\langle H_s \rangle, \langle H_d \rangle) & \text{if } Z \geq 50 \end{aligned} \quad (30)$$

$$\text{RMSD} = \left\{ \frac{\sum [BE_{exp}(N, Z) - BE_{th}(N, Z)]^2}{N_{nucl}} \right\}^{1/2}. \quad (31)$$

N_{nucl} is the number of nuclei for $N, Z \geq 8$. The minimization procedure uses the routine Minuit [21].

A. Macroscopic sector

The heavy task of the macroscopic sector is to ensure asymptotically a LD form and at the same time generate shell effects that move the HO closures to EI ones. As the Coulomb, asymmetry and pairing terms are already of LD type—within minor provisos—the task of generating shell effects falls on the first two terms in Eq. (23) in charge of bulk volume and surface contributions, as we have seen in Fig. 5. Table I follows the evolution of the fits as the coefficients are turned on. If we judge by these numbers, DZ10 does hardly better than any

TABLE I: The macroscopic coefficients, with their associated mean and RMS errors.

Op	a_i						
$M + S$	a_1	9.3980	5.2535	4.6971	16.6714	17.3653	17.5337
M/ρ	a_2	0.0000	-22.9448	-24.6563	11.8321	14.7737	15.4380
V_C	a_3	0.0000	0.0000	-0.0405	0.6680	0.6870	0.6946
V_T	a_4	0.0000	0.0000	0.0000	26.1232	35.6940	36.1628
V_{TS}	a_5	0.0000	0.0000	0.0000	0.0000	47.0442	48.4240
V_P	a_6	0.0000	0.0000	0.0000	0.0000	0.0000	5.0943
RMSD		64.062	29.190	29.063	4.232	2.934	2.852
mean		21.032	-2.222	-2.359	-0.163	-0.043	-0.053

standard LD fit. However, this is not an LD fit and surprises are in store. Fig. 6 displays the differences between the experimental and theoretical binding energies, calculated using only the macroscopic terms, Eq. (23). The pattern is both disconcerting and reassuring. It blows up at around $N \approx 80$ and there is no trace of the expected $A^{1/3}$ scaling. Things go much faster and the same time become nicely systematic. The scaling problem (the “original error” mentioned in Section IIE) can be traced to Section IIB where it was shown that different variants of the master term have the same shell effects but different asymptotics; the leading $M + S$ term in Eq. (19) has the correct asymptotics in A , no $A^{2/3}$ surface term and a $A^{1/3}$ part whose effects are sizeable (about 100 MeV around $A = 100$). The M/ρ surface contribution in Eq. (19)—which also contains HO shell effects—is left in charge of correcting the $A^{1/3}$ “drift”. An artificial procedure that explains the need of anomalous scalings but does not hide the systematic behavior they have to simulate.

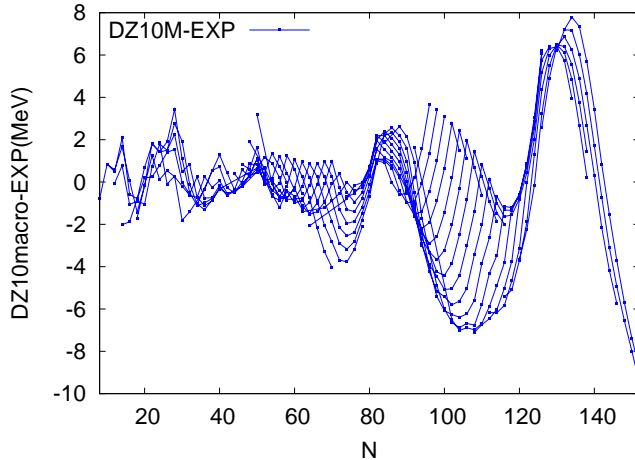


FIG. 6: Differences between the binding energies predicted by DZ10 macro, Eq. (23) and the experimental ones. Even-even nuclei (RMSD=2.86 MeV). Lines join points at constant $t = N - Z$

B. The microscopic sector

In Table II the full set of coefficients a_i , with their associated mean and RMS errors, is presented. All fits include the six macroscopic terms, plus some, or all, the microscopic ones, a_7 to a_{10} . It is clear that the three spherical terms can provide a reasonable good fit, with an RMSD of 0.72 MeV, but the three terms must be present, acting together. With only two of them the RMS error is larger than 2 MeV, as is the case if only the term associated with “deformed” nuclei is employed. When the 10 terms are active Eq. (30) fits the AME03 set with an RMSD of 0.55 MeV.

From the the discussion of Fig. 6 we understand both why anomalous scalings become necessary and why the terms of Eq. (28) manage to be so efficient. The factor $2\sqrt{p\nu} + \sqrt{p\pi}$ in Eq. (27), though atrocious, is a symptom of the difficulty of accommodating Fig. 6 with a single scaling. Eliminating it costs only some 50 keV. On the other hand, forcing the $A^{1/3}$ scaling leads to losses of some 200 keV. We shall examine closely the action of these terms in Section V.

C. The role of deformation

From the 2149 nuclei with masses reported in AME03 and $N, Z \geq 8$, 1827 are found to be spherical and 322 deformed. Figure 7 shows the DZ10 deformed and spherical binding

TABLE II: The full set of coefficients, with their associated mean and RMS errors.

Op	a_i						
$M + S$	a_1	17.492	17.542	17.769	17.778	17.770	17.766
M/ρ	a_2	15.284	15.507	16.258	16.355	16.210	16.314
V_C	a_3	0.693	0.694	0.708	0.708	0.707	0.707
V_T	a_4	35.513	35.721	38.354	37.480	38.080	37.515
V_{TS}	a_5	45.836	46.653	56.734	53.232	55.394	53.351
V_P	a_6	5.414	5.275	5.5361	6.373	5.269	6.199
s_3	a_7	0.062	0.448	0.000	0.390	0.000	0.478
s_3/ρ	a_8	0.000	2.106	0.000	1.763	0.000	2.183
s_4	a_9	0.000	0.000	0.0215	0.025	0.000	0.022
d_4	a_{10}	0.000	0.000	0.000	0.000	37.568	41.338
RMSD		2.443	2.293	2.028	0.717	2.280	0.554
mean		-0.040	-0.043	-0.035	0.002	-0.031	0.000

energies subtracted from the experimental ones for four chains of isotopes. The crossings signal the onset of deformation, which reproduces perfectly the N=90 transition region. Note as a pleasant result the correct inclusion of ^{130}Nd among deformed nuclei. It should be noted though that DZ10 underestimates the number of nuclei involved, as anticipated in Section II F and illustrated in Section V.

IV. PREDICTIVE POWER AND STABILITY OF DZ10

The quality of a fit depends not only on its RMSD but also on its error pattern: The closer the latter is to a uniform random distribution the better. As we have seen in Fig. 6, systematic deviations are not necessarily a bad thing. Strong isolated discrepancies are more serious. Figs. 8 shows that both effects are present in the full fit. To assess their impact we propose to follow some recent work [7] where a number of tests were introduced which probe the ability of nuclear mass models to extrapolate, all based on nuclear masses taken from ref. [4]. The tests are performed for the 2149 nuclei with $N \geq 8, Z \geq 8$ or the 1825 nuclei with $N \geq 28, Z \geq 28$. They are:

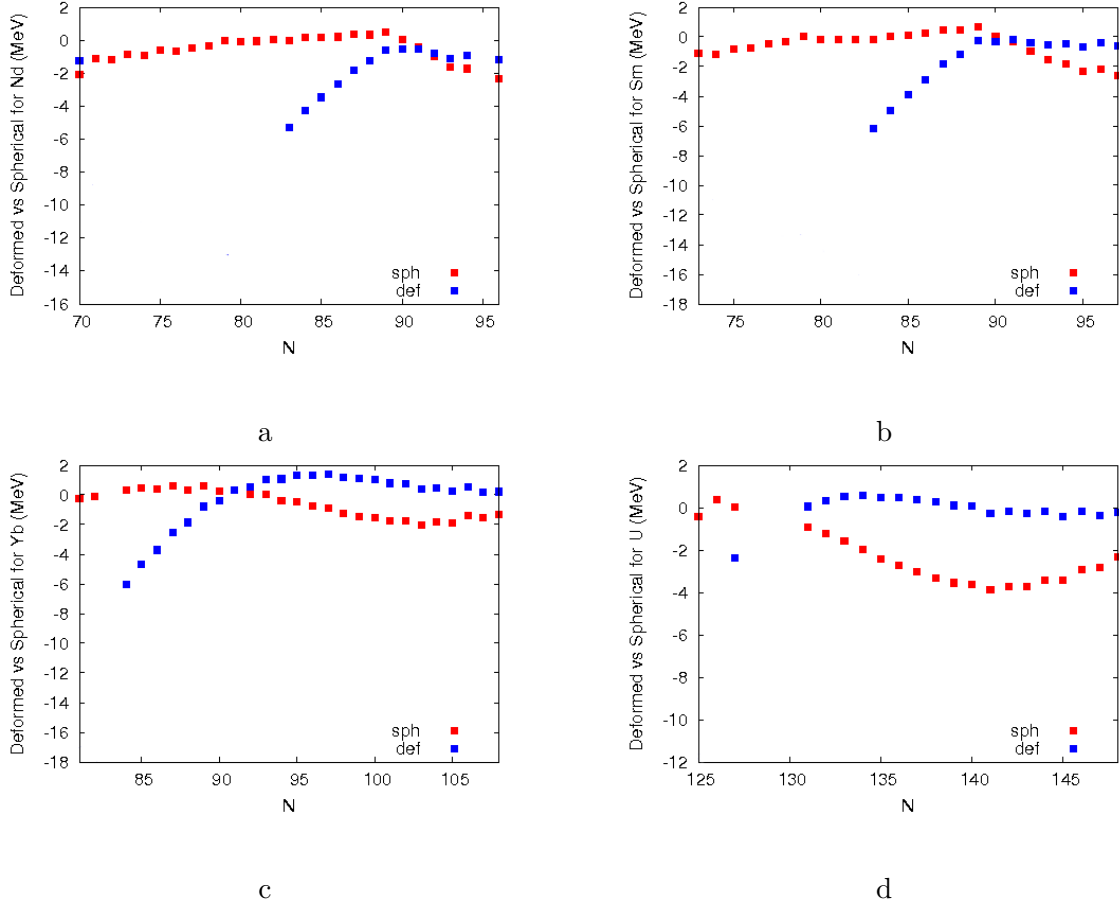


FIG. 7: Transition from spherical to deformed for the following chains of isotopes (a) Neodymium (${}_{60}\text{Nd}$); (b) Samarium (${}_{62}\text{Sm}$); (c) Ytterbium (${}_{70}\text{Yb}$) and (d) Uranium (${}_{92}\text{U}$).

- **AME95-03:** The subset of nuclei with measured masses in the AME95 compilation [5] is fitted. This test was used in ref. [3] to compare predictions of different models. In this work the actual masses used in the fit were taken from AME03, only the set of nuclei to be fitted is based on AME95.
- **Border region:** Nuclei which are furthest removed from stability are excluded from the fit and subsequently predicted by extrapolation.
- **Lead region:** Nuclei with mass number $A \leq 160, 170, 180, 190$ or 200 are fitted and the remaining ones, which always include the region around ${}^{208}\text{Pb}$, are predicted by extrapolation.

The number of nuclei with predicted masses ranges from 371 in AME95-03 to 810 for $A \leq 160$. The RMSD of the 16 fits are summarized in Table III. In the first line the

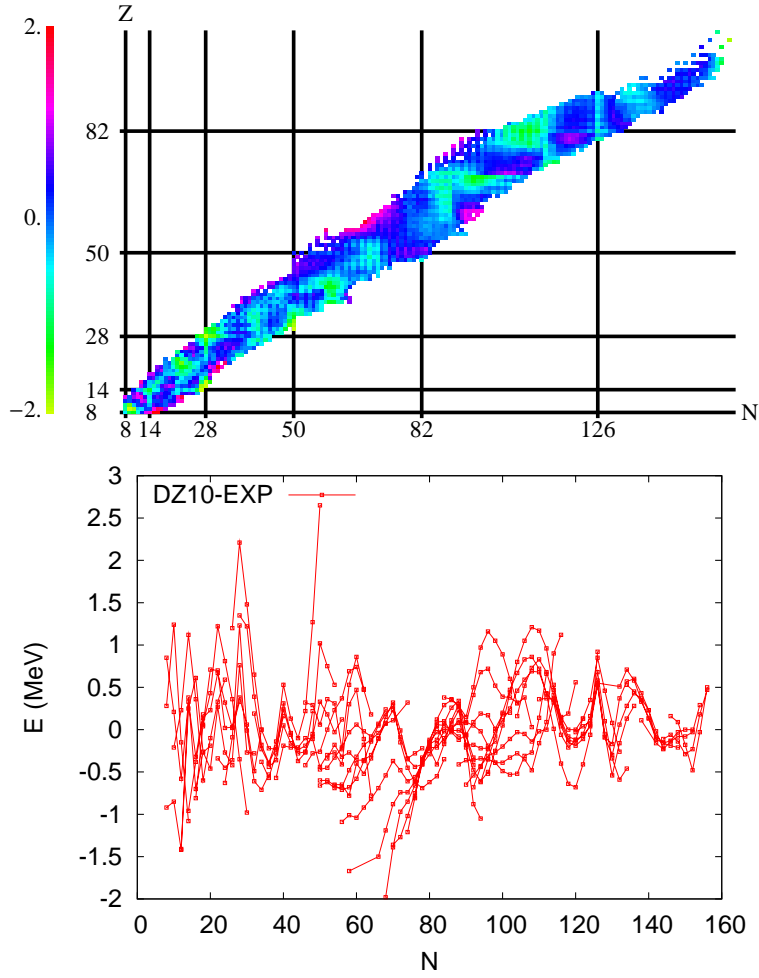


FIG. 8: Differences between the experimental binding energies and those calculated with the full fit. (RMSD= 0.55 MeV)

RMSD of the fits of the whole set of nuclei are presented. The fit is better when the lighter nuclei are excluded. Notice that, while the RMSD of the fits is slightly smaller for the subsets AME95 and border, as compared with the full set of nuclear masses, when the region around ^{208}Pb is excluded from the fit the RMSD are always larger. Also for the three subsets $A \leq 160, 170, 180$ the RMSD of the predictions is noticeably larger than the RMSD of the fits. The situation changes drastically for $A \leq 190, 200$, where the RMSD of the predictions are slightly smaller than those of the fits.

Associated with the 16 fits described above are 16 sets of coefficients $\{a_i\}$. They allow for a statistical analysis of their mean value, their root mean square deviation, and the percentage of variation, estimated as $100 \sigma / |mean|$. These numbers are reported in Table IV. In the first

TABLE III: RMSD of the different test applied to DZ10.

Test	$N, Z \geq 8$		$N, Z \geq 28$	
	fit	prediction	fit	prediction
Full set	0.5537		0.4819	
AME95-03	0.5076	0.7823	0.4469	0.6276
Border	0.4988	0.8212	0.4540	0.6527
$A \leq 160$	0.5787	0.9049	0.4823	1.2330
$A \leq 170$	0.5847	0.7740	0.4966	1.2889
$A \leq 180$	0.5708	0.7711	0.4859	1.0481
$A \leq 190$	0.5855	0.5611	0.5098	0.5010
$A \leq 200$	0.5844	0.5014	0.5054	0.4728

TABLE IV: Coefficients of the DZ10 mass formula obtained from the best fit of the full data set, their average, dispersion and fractional variation from the 16 fits.

Coefficient	a_1	a_2	a_3	a_4	a_5
full set	17.766	16.313	0.707	37.514	53.344
mean	17.773	16.332	0.707	37.327	52.277
σ	0.011	0.027	0.001	0.333	1.759
$100 \sigma / \text{mean}$	0.06	0.17	0.19	0.89	3.37
Coefficient	a_6	a_7	a_8	a_9	a_{10}
full set	6.1985	0.4784	2.1831	0.0216	41.3423
mean	6.2206	0.4853	2.1992	0.0218	40.6985
σ	0.1044	0.0426	0.2045	0.0006	1.4593
$100 \sigma / \text{mean}$	1.68	8.77	9.30	2.95	3.59

line the values obtained for the full fit of masses with $N, Z \geq 8$ are included for comparison. The six coefficients employed in the macroscopic terms vary less than 3%, the microscopic coefficients are found to vary up to 10%. In any case, it is clear that the DZ10 is very stable, with its coefficients varying smoothly and very moderately when the set of data employed in the fit is changed.

V. ANALYSIS OF THE ANOMALOUS EFFECTS

The anomalous spherical terms are conceptually unacceptable but phenomenologically crucial. To gain some insight into their behavior we choose five families of data with $t = N - Z = 8, 16, 24, 32$ and 40 , and examine how the macroscopic (macro) patterns are driven to reasonable agreement with the data (exp) in the full fit (dz10). Fig. 9 for $t = 8$ shows

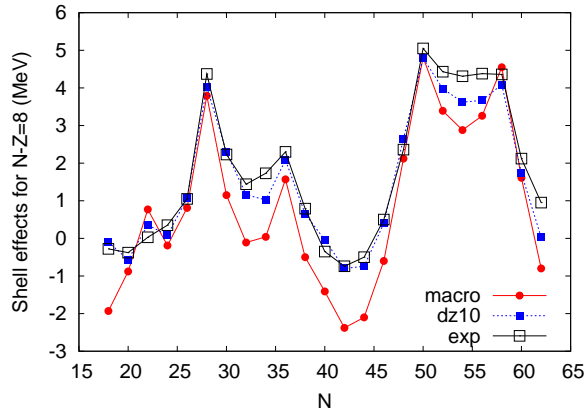


FIG. 9: Effect of anomalous terms for $N - Z = 8$ even-even nuclei referred to LD.

that macro comes close to the exp pattern but is slightly unbound. The anomalous terms bring in the necessary correction.

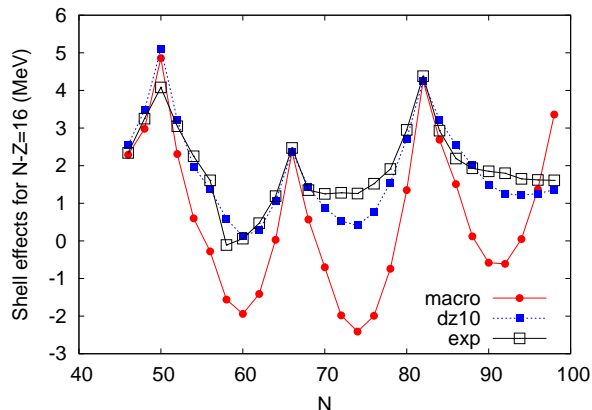


FIG. 10: Effect of anomalous terms for $N - Z = 16$ even-even nuclei referred to LD.

For $t = 16$ in Fig. 10 the situation changes dramatically: macro is way off except at the closures. Contrary to the $t = 8$ family where the naive shell model seems valid, most of the $t = 16$ nuclei exhibit vibrational features. In principle they would demand a separate

treatment as done for the well deformed species. As such a treatment remains to be found, DZ relies on the anomalous terms to restore reasonable agreement.

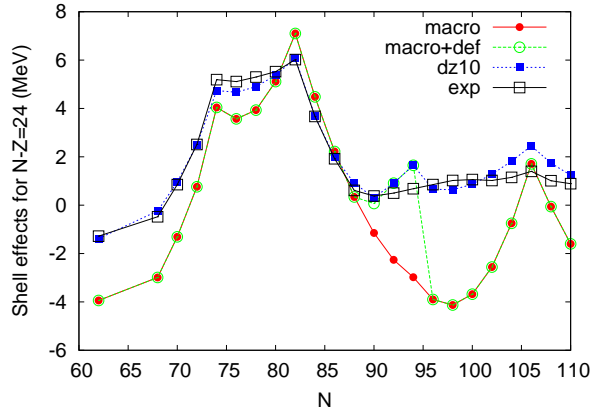


FIG. 11: Effect of anomalous terms for $N - Z = 24$ even-even nuclei referred to LD.

For $N - Z = 24$ in Fig. 11 the situation is more complicated: macro gives a good description near closures at $N = 82$ and $N = 106$, $Z = 82$ (^{188}Pb) but starts deviating strongly at $N = 90$ where deformation sets in. The inclusion of d_4 in Eq. (29) (macro+def in the figure) restores agreement with data for $N = 90, 92, 94$ that rapidly deteriorates at $N = 96$. The inclusion of the anomalous terms brings back reasonable agreement. This provides a clue that supplements what was found for $t = 16$.

DZ does an excellent job at describing the onset of deformation at $N = 90$ (^{156}Dy) through 4n-4p jumps, an idea vindicated by later work [12, 15, 20]. However, deformed regions not only start somewhere, they also end somewhere, in our case at the ^{188}Pb weak closure. In between, low lying γ bands indicate the need to go beyond 4n-4p jumps. DZ does not include this option and leaves the anomalous “spherical” terms in charge of deformation after d_4 fails to do it. Note that contrary to the $t = 16$ “vibrators” the necessary tools to go beyond 4n-4p jumps are available, as explained in Section II F.

Something similar occurs for $N - Z = 32$ in Fig. 12: macro is good at first, then deformation sets in and is well described by def for a while but then the anomalous terms take over in a region that remains well deformed. They even correct nicely what is missed by macro at the $N = 114$, $Z = 82$ closure. The situation becomes baffling for $t = 40$ in Fig. 13 because of the uncanny capacity of the anomalous terms to restore agreement with data that appeared compromised by the distorted macroscopic pattern.

The anomalous terms can deal with practically everything, including deformation. This

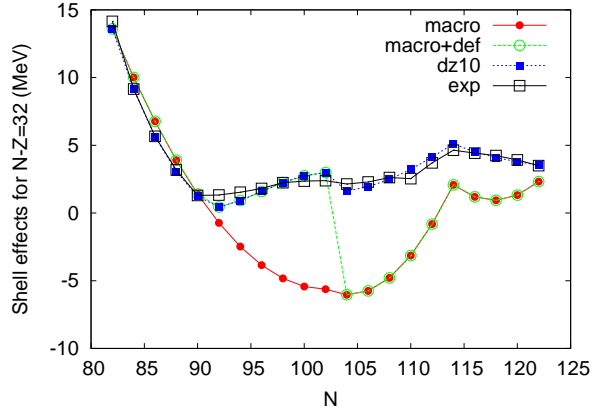


FIG. 12: Effect of anomalous terms for $N - Z=32$ even-even nuclei referred to LD.

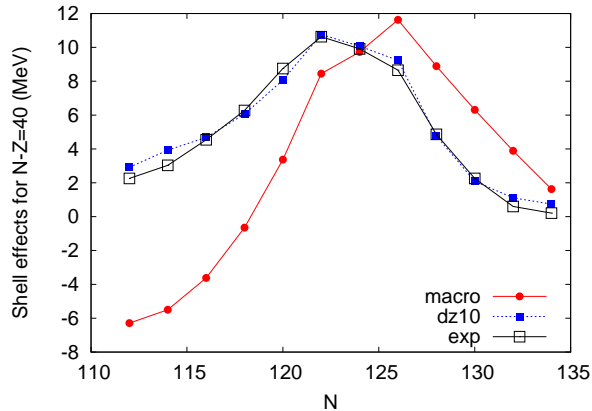


FIG. 13: Effect of anomalous terms for $N - Z=40$ even-even nuclei referred to LD.

is achieved by borrowing the sound idea of simple polynomial forms and subverting it by introducing unacceptable scalings. Among the many things they do, the anomalous terms correct shortcomings of the macroscopic contribution, as seen in the $Z = 82$ closure for $t = 32$ and in the $t = 40$ case. We have already traced the scaling flaws of the macroscopic terms in the discussion of Fig. 6 but its worth pushing their analysis in a totally different direction.

VI. ANALYSIS OF THE MACROSCOPIC TERM. GEMO

Rather than attempting to correct directly the scaling flaws of DZ10, we shall compare the model with a complementary approach in which it is very simple to force correct asymptotics, and has the enormous advantage of being practically parameter free.

Ideally, the macroscopic-microscopic separation should mirror the monopole-multipole separation of the realistic interactions [10, 11, 15]. We recall that the monopole part provides the natural definition of the unperturbed Hamiltonian as it contains all the number and isospin operators and all that is needed for a spherical Hartree Fock variation. Our purpose is to examine to what extent the macroscopic DZ10 terms are consistent with a monopole Hamiltonian derived without any reference to masses; defined in [22] (DZII or GEMO (GEneral MOnopole) after the name of the code [8, under item containing [22]]) by fitting (quite well) all single particle and single hole states on doubly magic nuclei (the $cs \pm 1$ set). Some details that supplement the original paper can be found in [12, 15]. GEMO is fully equivalent to a mean field calculation of monopole shell effects. It decouples approximately the macroscopic part by replacing the master term by the combination $M_A - 4K$ which has no A and $A^{2/3}$ contributions and produces shell effects similar to those of Fig. 3. M_A is from Eq. (2) and K is the kinetic energy affected by an $\hbar\omega_0 \approx 11$ denominator chosen to reproduce the correct coefficient for the $M_A - 4K$ term.

$$K = \frac{\hbar\omega}{2\hbar\omega_0} \sum_p m_p(p + 3/2) \implies \frac{\hbar\omega}{4\hbar\omega_0} (p_f + 3)^3 (p_f + 2) \quad (32)$$

Asymptotically we obtain from a fit $(M_A - 4K) \asymp -28.04A^{1/3} - 9.15t^2/A + 9.43$; and from now on GEMO stands for the properly subtracted value. To compare with experiment *we subject GEMO to a 2.5 contraction* (the only free parameter, to be examined later) and we add to it $E(LD)$ from Eq.(1). In the calculation the filling order of the orbits has been

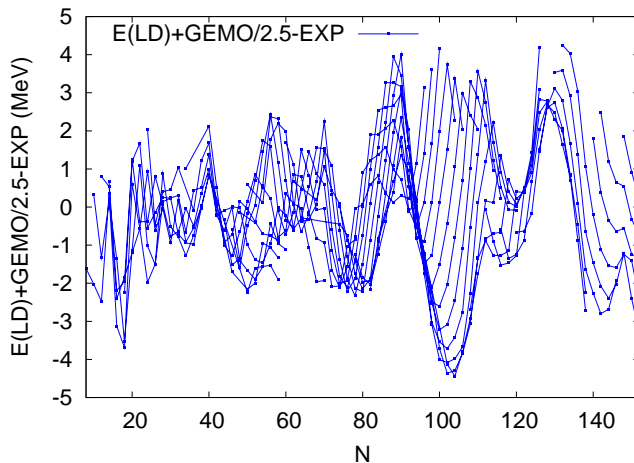


FIG. 14: Comparison between GEMO and experimental masses for even-even nuclei. RMSD=1.69 MeV. Lines join points at constant $t = N - Z$. See text

kept fixed throughout, according to an $l \cdot s$ law with an $l \cdot l$ modulation. Much better results are expected if the proper procedure is followed by determining variationally the filling order for each nucleus. In spite of this shortcoming the results shown in Fig. 14 have substantially smaller RMSD than those for DZ10 in Fig. 6 (1.69 *vs* 2.86 MeV. Beware of y-scale differences between the figures). However, for $N \lesssim 80$ both models have very much the same RMSD ≈ 1.2 MeV. The difference is entirely due to a flatter GEMO pattern (*i. e.*, more symmetric around the origin), consistent with $A^{1/3}$ scaling. In the lighter region it is impossible to identify common systematics, while the heavier one is dominated by cubic parabolic trends, *e. g* in the EI space between $N = 82$ and 126.

If we now compare the models for the cases studied in last section we find the following; at $t = 8$ GEMO is better, at $t = 16$ DZ10macro is better, at $t = 24$ and 32 both are comparable provided the filling orders are corrected, at $t = 40$ GEMO is much better. In general, the detailed subshell structure of GEMO is a source of unphysical, jumpy, behaviour (common to mean field formulations), while DZ10macro suffers from distortions due to bad asymptotics; but both models are telling the same thing about anomalous terms:

- Bad scaling is due to bad asymptotics.
- Cubic terms *i.e.*, three body forces are a fact, not a DZ10 artifact. In the next section we shall offer a proof of the need of genuine three body forces to explain the HO-EI transition.

Let us conclude with a word on the 2.5 contraction. GEMO was fitted to single particle and single hole properties on closed shell nuclei: they demand huge shell effects whose relative positions are little affected by total binding energies *i. e.*, by correlation effects. Once these are switched on they will produce in first approximation parabolas of negative slope $m(D - m)$ opposite to those in, say, Fig. 3, of form $m(m - D)$. The contraction factor simulates this mechanism. The argument is purely heuristic—we have not specified the nature of the correlations—but conceptually valuable as it provides an estimate of their (large) magnitude and explains the impossibility for an effective mean field description to describe simultaneously masses and single particle or single hole energies on closed shells. In DZ10 the correlation effect is directly incorporated in a single master term that produces both shell effects and the bulk energy of nuclear matter. A non trivial achievement.

VII. REALISTIC FORCES AND THE THREE BODY ISSUE

The DZ strategy amounts to assume perfect potentials and proceed as if we were solving the Schrödinger equation. A perfect potential should saturate *i.e.*, produce the correct energies at the right radii. It should also produce the EI closures. It does neither. Therefore DZ postulates that the necessary mechanisms can be incorporated into some effective master terms M_A and M_T and adopts the standard shell model approach of “freezing” $\hbar\omega$ at the observed radii. The present consensus [15, 18] demands the introduction of three body forces, and in recent years considerable effort has been devoted to derive them from chiral perturbation theory, with some success as witnessed by a recent paper [23] where abundant references will be found. However, much remains to be done at the fundamental level and here we shall follow the policy of consulting the data searching for hints about the monopole Hamiltonian. Our first task is to identify the form of the necessary three body terms.

NOTATIONS: in what follows we use $X_{st} = X_s(X_t - \delta_{st})/(1 + \delta_{st})$; $X^{(2)} = X(X - 1)$.

We start with an isoscalar monopole two body interaction written as $H_m = \sum_{s \leq t} m_{st} V_{st}$ where the sums extend over all orbits st . From now on we omit the V_{st} matrix elements and consider only the m_{st} operators. Next we examine the action of H_m in a major HO shell, and call c the occupied (“core”) orbits below the major shell. It will give three types of contribution: $m_{cc'} = D_{cc'}$, $m_c m_s = D_c m_s$ and m_{st} , where we have replaced the core occupancies by the degeneracies D_c of the corresponding orbits. We are left with a pure core contribution that we assume will be taken care of by the master term, an effective single particle term in m_s and the genuine two body m_{st} part.

The first key step is to adopt the “invariant representation” [24, and references therein]. An early—relatively successful but inconclusive—attempt to introduce many body forces] to separate the total number operator m_p in HO shell p from others that are taken to be “orthogonal” to it in the sense that they vanish for $m_p = 0$ and $\bar{m}_p = D_p - m_p = 0$ *i.e.*, for zero particles and zero holes. This is achieved as follows (the orbit 1 can be chosen arbitrarily),

$$m_s \equiv m_p + \Gamma_{s1}^{(1)} \tag{33}$$

$$m_{st} \equiv \frac{1}{2} m_p^{(2)} + (m_p - 1) \Gamma_{s1}^{(1)} + \Gamma_{st}^{(2)}, \tag{34}$$

where

$$\Gamma_{s1}^{(1)} = \left(\frac{m_s}{D_s} - \frac{m_1}{D_1} \right) \frac{D_s D_1}{D_s + D_1} = - \left(\frac{\bar{m}_s}{D_s} - \frac{\bar{m}_1}{D_1} \right) \frac{D_s D_1}{D_s + D_1} = -\bar{\Gamma}_{s1}^{(1)} \quad (35)$$

$$\Gamma_{st}^{(2)} = \left(\frac{m_s^{(2)}}{D_s^{(2)}} + \frac{m_t^{(2)}}{D_t^{(2)}} - \frac{2m_s m_t}{D_s D_t} \right) \frac{D_s^{(2)} D_t^{(2)}}{(D_s + D_t)^{(2)}} = \bar{\Gamma}_{st}^{(2)} \equiv \Gamma_{st}^{(2)}(\bar{m}_s, \bar{m}_t) \quad (36)$$

In reading these expressions it is convenient to fix ideas through an example. Consider the *sd* shell. Eq. (33) gives the spectrum of ^{17}O . The m part belongs to the master term. The single particle energies are referred to one of them through $\Gamma_{s1}^{(1)}$ operators in Eq. (35) which change sign when particles are turned into holes in ^{39}Ca . The normalization ensures unit splitting between single particle states s and 1. The $m_p^{(2)}$ in Eq. (34) goes with the master term. Then we have a modulation of the single particle energies $(m_p - 1)\Gamma_{s1}^{(1)}$ that makes it possible for the splittings in ^{39}Ca to be different from those in ^{17}O . Finally the $\Gamma_{st}^{(2)}$ operators which according to Eq. (36) are particle-hole symmetric and vanish for $m, \bar{m} = 0, 1$. They reproduce the strictly two body contributions to the centroids (average energies) of two particle and two hole configurations. The normalizations are such as to produce splittings of order one between the centroids.

The second key step is as metaphysical as physical: to select very few possible operators. If too many are truly needed, our approach is doomed. Much of the success of DZ is due to the choice of a single $\Gamma_p^{(1)} = \Gamma_{j(p)r(p)}^{(1)}$. This may do for masses, but a general H_m needs some extra freedom. As any one body operator referred to its centroid becomes “strict one body” in the sense that it vanishes at both $m_p, \bar{m}_p = 0$ two classical choices come to mind $l \cdot s$ and $l \cdot l \equiv l(l+1) - p(p+3)/2$ (they may be written as combinations of $\Gamma_{s1}^{(1)}$ [22]). For the strict two body case the only obvious choice is $\Gamma_p^{(2)} = \Gamma_{j(p)r(p)}^{(2)}$. For simplicity, in what follows we refer to a single generic $\Gamma_p^{(1,2)}$.

So far we have considered one major HO shell. In general, particles may move in different shells. The possible cross shell operators will be of the form

$$m_p m_{p'}, m_p \Gamma_{p'}^{(1)}, \Gamma_p^{(1)} \Gamma_{p'}^{(1)}.$$

Upon introducing three body interactions we shall encounter terms of the type

$$m_{cc'c''} \equiv D_{cc'c''}, m_{cc'} m_s \equiv D_{cc'} m_s \text{ and } D_c m_{st}$$

which will modify the two body equations (33,34). The genuine m_{stu} parts will contain m_p , and $\Gamma_p^{(1,2)}$ operators plus eventually cubics $\Gamma_p^{(3)}$. By now we can propose a list of possible

operators:

$$\text{intra shell : } (a_1 + b_1 m_p + c_1 m_p^2) \Gamma_p^{(1)}, \quad (a_2 + b_2 m_p) \Gamma_p^{(2)}, \quad a_3 \Gamma_p^{(3)} \quad (37)$$

$$\text{cross shell : } (\alpha_1 m_p + \beta_1 m_p^2 + \gamma_1 m_p m_{p'}) \Gamma_{p'}^{(1)}, \quad m_p (\alpha_2 \Gamma_{p'}^{(2)} + \beta_2 \Gamma_p^{(1)} \Gamma_{p'}^{(1)}), \quad \alpha_3 \Gamma_p^{(1)} \Gamma_{p'}^{(2)} \quad (38)$$

We should not forget the pure m contributions that we have decided to ascribe to (the three body part of) the master term, see [15, p 437] for some speculation on the subject.

Everything we have said applies either to purely isoscalar operators or to a neutron proton representation, in which case each major shell is split in two with m_s replaced by n_s and z_s . Physically it is preferable to work in an isospin representation involving m_s and T_s operators. The reason can be understood by referring to Fig. 1 which shows that shell effects are very much the same for both fluids (at constant N or Z). If we plot along lines of constant A or T , the former become the fairly smooth “ β decay parabolas” while the latter (of which we have seen many examples) exhibit most of the shell structure, indicating its basically isoscalar character. Let us examine how to proceed.

A. The origin of the HO-EI transition

Once we accept that three body effects are necessary, we must find ways to identify the relevant operators. As there are several candidates, to select them by fitting masses may give non unique answers. The best way to proceed—as far as the HO-EI transition is concerned—is to look into spectroscopic information: an apparently impossible task that turns out to be very simple.

The unequivocal sign that a strict two body treatment is not sufficient came from exact calculations leading to a $J^\pi = 1^+$ ground state of ^{10}B instead of the observed 3^+ [25, 26], a long standing puzzle in conventional shell model work, where exactly the same problem exists in ^{22}Na . Then it was shown [27] that by changing the V_{jj}^T , V_{jr}^T centroids of a realistic interaction R according to

$$\begin{aligned} V_{jr}^T(\text{R}) &\implies V_{jr}^T(\text{R}) - (-)^T \kappa \\ V_{jj}^T(\text{R}) &\implies V_{jj}^T(\text{R}) - 1.5 \kappa \delta_{T,0} \end{aligned} \quad (39)$$

one could correct much of the spectroscopic trouble in the p , sd and pf shells. To within some fine tunings—and a major difference—this is a time-honored two body prescription [28]

that has become a common feature of effective interactions in the pf shell [15, sections V, VB]. The major difference is that κ is a linear function of m_p , which makes the prescription three body. But it (still) has a flaw: as it was originally devised to ensure EI closures at ^{48}Ca and ^{56}Ni where the V_{rr}^T centroids play no role, they were left out. To include them we note

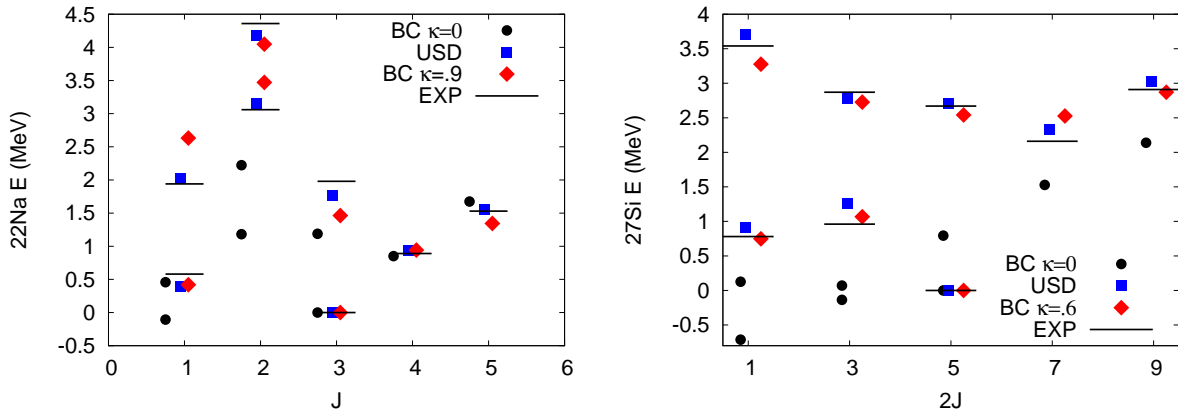


FIG. 15: Spectra of ^{22}Na and ^{27}Si . The uncorrected and corrected Bonn C interaction (BC) [29] is compared with USD [30] and experiment.

that the six centroids involved, once cast as three isoscalar and three isovector terms, reduce to four by removing the overall $m(m-1)$ and $T(T+1)$ dependences. According to our policy of omitting at first the isovector pieces, we are left with the terms in Eq. (37). We ignore the last and redo the calculations in [27]. We know from [24] that $(a_1 + b_1 m_p + c_1 m_p^2)\Gamma_p^{(1)}$ plays a role, but it does not solve the problems. Therefore we simulate its influence by pushing up the $d_{3/2}$ orbit two MeV above its observed value (arbitrary move but of little consequence). We are left with $(a_2 + b_2 m_p)\Gamma_{j(p)r(p)}^{(2)} \equiv \kappa(m)\Gamma_{j(p)r(p)}^{(2)}$, which is seen in Fig. 15 to work very well: the dismal spectra produced by the original interaction (Bonn C $\kappa=0$) become adequate in ^{22}Na (Bonn C $\kappa(6) = 0.9$) and good, even when compared with USD, in ^{27}Si (Bonn C $\kappa(11) = 0.6$). There is no way to find a compromise, constant, κ .

A refined approach will demand the inclusion of some other operators, but there are reasons to believe that $\kappa(m)\Gamma_p^{(2)}$ will play a (the) fundamental role in the HO-EI transition.

VIII. HOMAGE TO JEAN DUFLO AND CONCLUSIONS

In all justice DZ10 should be called D10 because it was entirely the work of the late Jean Duflo. It was designed to shed some light on the problems of DZ28:

a) Too many parameters; b) Obscure origin of EI closures; c) Many surface terms that lead to a change of sign at around $A = 120$; d) Anomalous A scalings.

At the price of a substantial but acceptable RMSD increase, Duflo solved a, clarified b, reduced c to a single three body term and was left with d. He had a genius for regrouping and eliminating theoretically plausible contributions and inventing phenomenological ones demanded by data. Jean was a magical data manager. He was also aware that DZ10 needed improvements, and to the last day he worked on them. He did not find a satisfactory solution, but from his notes one could guess that he did not worry about anomalous terms and concentrated on basic shell formation. Our present work points to the same direction. We have explained how the scaling anomaly can be eliminated and demonstrated the need of genuine three body forces. It remains to be seen whether these advances can lead to a formulation as compact and successful as D10.

Acknowledgments

We have enjoyed some interesting exchanges at GSI and Darmstadt with H. Feldmeier, G. Martínez Pinedo, N. Pietralla and F. Thielemann. Special thanks are due to the referee whose remarks lead to substantial improvements. This work was supported in part by Conacyt, México, by FONCICYT project 94142, by DGAPA, UNAM and by Helmholtz Alliance HA216/EMMI.

-
- [1] C.E. Rolfs and W.S. Rodney, *Cauldrons in the Cosmos* (University of Chicago Press, Chicago, 1988).
 - [2] Klaus Blaum, Phys. Rep. **425** (2006) 1.
 - [3] D. Lunney, J.M. Pearson, C. Thibault, Rev. Mod. Phys. **75** (2003) 1021.
 - [4] G. Audi, A.H. Wapstra, C. Thibault, Nucl. Phys. **A 729** (2003) 337.
 - [5] G. Audi, A.H. Wapstra, C. Thibault, Nucl. Phys. **A 595** (1995) 409.
 - [6] J. Duflo and A.P. Zuker, Phys. Rev. C **52** R23 (1995) R23.
 - [7] J. Mendoza-Temis, I. Morales, J. Barea, A. Frank, J.G. Hirsch, J.C. López-Vieyra, P. Van Isacker and V. Velázquez, Nucl. Phys. **A 812** (2008) 28.

- [8] <http://amdc.in2p3.fr/web/dz.html>
- [9] J. Duflo, Nucl. Phys. **A 576** (1994) 29.
- [10] A.P. Zuker, Nucl. Phys. **A 576** (1994) 65.
- [11] M. Dufour, A.P. Zuker, Phys. Rev. C **54** 1641 (1996).
- [12] A.P. Zuker, Rev. Mex. Fis. S **54** (2008) 129, Corrected (recommended) version in site [8];
- [13] A. Bohr, B.R. Mottelson, *Nuclear Structure, Vol. I: Single-Particle Motion*, World Scientific, Singapore (1998), Sect. 2-4.
- [14] J. Duflo, A.P. Zuker, Phys. Rev. C **59** 051304R (2002).
- [15] E. Caurier, G. Martínez-Pinedo, F. Nowacki, A. Poves, A. P. Zuker, RMP **77**, pags. 427-488 (2005); <http://arxiv.org/pdf/nucl-th/0402046>
- [16] D. R. Entem and R. Machleidt, Phys. Rev. C **68**, 041001 (2003)
- [17] S. K. Boegner, T. T. S. Kuo, A. Schwenk, Phys. Rep. **386**, 1 (2003)
- [18] A. Schwenk and A. P. Zuker, Phys. Rev. C **74**, 061302(R) (2006).
- [19] A. P. Zuker, S. Lenzi, Gabriel Martínez Pinedo and A. Poves, Phys. Rev. Lett. **89**, 142502 (2002).
- [20] A. P. Zuker, J. Retamosa, A. Poves and E. Caurier, Phys. Rev. C **52** R1741 (1995).
- [21] F. James, Minuit: Function Minimization and Error Analysis Reference Manual, Version 94.1, CERN (1994); <http://wwwasdoc.web.cern.ch/wwwasdoc/minuit/minmain.html>
- [22] [GEMO] J. Duflo, A.P. Zuker, Phys. Rev. C **59** R2347 (1999).
- [23] T. Otsuka, T. Suzuki, J. H. Holt, A. Schwenk and Y. Akaishi; <http://arxiv.org/pdf/0908.2607v1>
- [24] A. Abzouzi, E. Caurier and A. P. Zuker, Phys. Rev. Lett. **66** 1134 (1991).
- [25] P. Navratil and W. E. Ormand, Phys. Rev. Lett. **88** 152502 (2002).
- [26] S. C. Pieper, K. Varga and R. B. Wiringa, Phys. Rev. C **66** 044310 (2002).
- [27] A. P. Zuker, Phys. Rev. Lett. **90**, 042502 (2003).
- [28] E. Pasquini, Ph.D. thesis, Report No. CRN/PT 76-14, Strasbourg, 1976. E. Pasquini and A. P. Zuker in *Physics of Medium Light Nuclei*, Florence, 1977, edited by P. Blasi and R. Ricci (Editrice Compositrice, Bologna, 1978).
- [29] M. Horth-Jensen, T. T. S. Kuo and E. Osnes, Phys. Rep. **261**, 126 (1995).
- [30] B. H. Wildenthal, Prog. Part. Nucl. Phys. **11**, 5 (1984).